

## Local Thermal Expansion in a Cuprite Structure: The Case of Ag<sub>2</sub>O

S. a Beccara, G. Dalba, P. Fornasini,\* R. Grisenti, and A. Sanson

*Istituto Nazionale per la Fisica della Materia and Dipartimento di Fisica, Università di Trento, I-38050 Povo (Trento), Italy*

F. Rocca

*IFN, Istituto di Fotonica e Nanotecnologie del Consiglio Nazionale delle Ricerche,*

*Sezione CeFSA di Trento - 38050 Povo (Trento), Italy*

(Received 30 April 2002; published 20 June 2002)

The local thermal behavior of the Ag<sub>2</sub>O framework structure has been studied by extended x-ray absorption fine structure. The average Ag-O nearest-neighbor distance expands upon heating, while the Ag-Ag next-nearest-neighbor distance contracts. An original implementation of the cumulant analysis shows that the Ag-O expansion is a joint effect of potential anharmonicity and geometrical deformation of the Ag<sub>4</sub>O basic tetrahedral units. Accordingly, the negative thermal expansion of the lattice parameter in Ag<sub>2</sub>O cannot be explained uniquely in terms of rigid unit modes.

DOI: 10.1103/PhysRevLett.89.025503

PACS numbers: 63.20.Ry, 65.40.-b, 87.64.Fb

Silver oxide Ag<sub>2</sub>O shares with copper oxide Cu<sub>2</sub>O the cuprite structure (space group  $Pn\bar{3}m = O_h^4$ ), in which each  $M$  atom ( $M = \text{Cu}, \text{Ag}$ ) is linearly coordinated to two O atoms, and each O atom is tetrahedrally coordinated to four  $M$  atoms. The cuprite structure can be described as a framework of two interpenetrating but independent networks of corner-sharing  $M_4\text{O}$  tetrahedra [1]. Cu<sub>2</sub>O and Ag<sub>2</sub>O have been studied for several decades, due to their peculiar electronic and dynamic properties [2,3]. The shear stiffness coefficients, measured for Cu<sub>2</sub>O and calculated for Ag<sub>2</sub>O, are unusually low, and increase with temperature. The cell parameter of Cu<sub>2</sub>O contracts when temperature is raised from liquid helium up to 200 K and is nearly constant from 200 to 300 K [4,5]. A negative thermal expansion (NTE) has been recently measured also for Ag<sub>2</sub>O from 10 to 450 K [6].

NTE extending over large temperature ranges is frequently observed in framework structures [7]. Much interest has been recently aroused by ZrW<sub>2</sub>O<sub>8</sub>, whose lattice parameter regularly contracts from 0.3 to 1050 K [8]. Explaining NTE in terms of local structure and dynamics represents a challenging basic problem. The thermal expansion of framework structures results from the competition between a positive contribution of the potential anharmonicity and a negative contribution which is often attributed to a network folding induced by low frequency rigid unit modes (RUM) [9]. Although elegant and appealing, RUM theories still lack some relevant experimental checks. To this aim, it is important to directly measure the thermal expansion of nearest-neighbor bonds and the degree of rigidity of corner-sharing basic units. If low-frequency librational modes of rigid units are present in a crystal, the nearest-neighbor distance measured by Bragg diffraction is shorter than the average bond distance [10]. Attempts at assessing the bond thermal expansion in silicates [11] and in ZrW<sub>2</sub>O<sub>8</sub> [12] have been done through a refinement of Bragg spectra based on TLS

(translation, librations, and screw) models, which however *a priori* assume the rigidity of the basic units [10]. In a more effective recent approach, the analysis of total neutron scattering allows one to exploit the information on the correlation embedded in thermal diffuse scattering [13,14].

In this Letter we demonstrate that original experimental information on the local thermal properties of framework structures can be obtained by extended x-ray absorption fine structure (EXAFS). In particular, the thermal expansion of the nearest-neighbor distance is directly measured and the deformation of the basic units can be detected.

Easiness of temperature dependent measurements, selectivity of atomic species, and insensitivity to long range order make EXAFS particularly suited to study the thermal properties of the first coordination shells of a given x-ray absorbing atom, particularly high being the accuracy for the nearest-neighbor 1st shell. Position, width, and shape of the distributions of interatomic distances can be determined from EXAFS through a data analysis based on the cumulant expansion method [15,16], which yields the lowest order cumulants  $C_i^*$  of the distribution for each coordination shell. First and second cumulants are average value and variance of the distribution, respectively. Higher order cumulants describe the deviation from the Gaussian shape as the effect of anharmonicity; in particular, the third cumulant measures the distribution asymmetry. Neglecting the third cumulant leads to wrong values of the interatomic distance. EXAFS is sensitive to the correlation of atomic thermal motion, measured by the mean square relative displacement (MSRD), which is conveniently decomposed into its projections parallel and perpendicular to the average bond direction [17]:  $\langle \Delta u^2 \rangle = \langle \Delta u_{\parallel}^2 \rangle + \langle \Delta u_{\perp}^2 \rangle$ . The second cumulant corresponds to a good approximation to the *parallel* MSRD,  $C_2^* \approx \langle \Delta u_{\parallel}^2 \rangle$ .

While Bragg diffraction measures the distance between average atomic positions, EXAFS, due to its sensitivity to

correlation, measures the average interatomic distance, like diffuse scattering. The main advantage of the cumulant analysis of EXAFS over the conventional analyses of diffuse scattering is the ability to distinguish between anharmonicity and geometrical effects. To elucidate this point, let us recall the relations between EXAFS cumulants and MSRDs [16]. To deal with framework structures, we here extend the treatment from the well established case of pure translational motion to the case of pure librational motion. Let  $R_0$  be the interatomic distance in an ideal classical crystal frozen at 0 K. The instantaneous bond distance is, to first approximation,

$$r \simeq R_0 + \Delta u_{\parallel} + \Delta u_{\perp}^2/2R_0. \quad (1)$$

Relying on the quasiharmonic approximation, the second term on the right can be decomposed as  $\Delta u_{\parallel} = a + (\Delta u_{\parallel})_h$ , where  $a$  is the thermal expansion due to the anharmonicity of the effective pair potential, while  $(\Delta u_{\parallel})_h$  is a harmonic contribution. The first EXAFS cumulant is the average interatomic distance,  $C_1^* = \langle r \rangle$ ; let us find its relation with the crystallographic distance  $R_c$  measured by Bragg diffraction. For a pure *translational* relative motion, the three-dimensional harmonic distribution of relative distances is an ellipsoid, so that  $\langle \Delta u_{\parallel} \rangle_h = 0$ , and

$$C_1^* \simeq R_0 + a + \langle \Delta u_{\perp}^2 \rangle / 2R_0; \quad R_c = R_0 + a. \quad (2)$$

For a pure *librational* motion, the ellipsoid is curved along a spherical surface (the *banana effect* [10]), so that  $\langle \Delta u_{\parallel} \rangle_h \simeq -\langle \Delta u_{\perp}^2 \rangle / 2R_0$ , and

$$C_1^* = R_0 + a; \quad R_c \simeq R_0 + a - \langle \Delta u_{\perp}^2 \rangle / 2R_0. \quad (3)$$

It is worth noting that  $a$  and  $\langle \Delta u_{\perp}^2 \rangle$  have finite values at zero kelvin, reflecting the effect of zero point motion. In both cases of translation and libration,  $C_1^* \simeq R_c + \langle \Delta u_{\perp}^2 \rangle / 2R_0$ . In agreement with Eq. (2), a larger thermal expansion has been measured by EXAFS in several crystals with respect to diffraction [18,19]. In the case of germanium, the 1st-shell *perpendicular* MSRD  $\langle \Delta u_{\perp}^2 \rangle$  was determined by comparing the EXAFS and crystallographic thermal expansions [20].

According to Eq. (3), for a pure librational motion the bond thermal expansion measured by the 1st EXAFS cumulant is entirely due to the anharmonicity of the effective potential:  $\delta C_1^* = \delta a$ . A procedure for connecting the quantity  $a$  to the 2nd and 3rd EXAFS cumulants has been developed by Frenkel and Rehr [21] on the basis of a perturbative quantum approach in quasiharmonic approximation and has been successfully tested for the 1st shell of germanium [20]. In the case of framework structures, this procedure gives the possibility of directly comparing  $\delta C_1^*$  with  $\delta a$ , thus evaluating the degree of rigidity of the basic units.

Contrary to other framework structures, in crystals with the cuprite structure the cations, which are more suited than oxygen for accurate EXAFS studies, are at the corners of the tetrahedral units. This allows one to obtain significant

information not only about 1st-shell nearest neighbors, but also about 2nd-shell next nearest neighbors. The choice of  $\text{Ag}_2\text{O}$  is related to a research program on fast-ion-conducting silver-borate glasses in which  $\text{Ag}_2\text{O}$  is present as modifier oxide [22].

In this Letter we present the results of EXAFS measurements performed at the  $K$  edge of silver in  $\text{Ag}_2\text{O}$ , in the temperature range from 7 to 500 K. A homogeneous sample was prepared by depositing a  $\text{Ag}_2\text{O}$  powder on a polytetrafluoroethylene membrane. The sample thickness was chosen so as to have an edge jump  $\Delta\mu x \simeq 1$  at the  $K$  absorption edge of silver. EXAFS was measured in transmission mode at the beam line BM08 (Gilda) of ESRF (European Synchrotron Radiation Facility), Grenoble, using a silicon crystal with (311) reflecting faces. At least two spectra were collected at each temperature. The EXAFS signals were extracted from the experimental spectra, after a careful alignment of the energy axis, according to well established procedures [23]. The Fourier transforms of EXAFS signals are shown in Fig. 1 for selected temperatures.

The peak between 1 and 2 Å in Fig. 1 corresponds to the 1st coordination shell of Ag (two oxygens at 2.04 Å). The 1st-shell contributions to EXAFS at different temperatures, obtained by Fourier backtransform, were analyzed by the method of phase difference and amplitude ratio (*ratio method*) [15,16], using the 7 K spectra as reference for backscattering amplitude, phase shifts, and inelastic terms. The structure between 2 and 4 Å in Fig. 1 contains the single scattering contributions of both 2nd and 3rd shells of Ag (12 Ag at 3.34 Å and 6 O at 3.91 Å, respectively) together with possible multiple scattering (MS) effects. A simulation performed with the FEFF code [24] allowed us to assess that MS contributions are negligible and to evaluate the relative importance of 2nd and 3rd shell cumulants.

The relative values of the first four cumulants  $\delta C_i = C_i(T) - C_i(7\text{K})$  of an *effective* distribution of distances were the results of EXAFS analyses for both the 1st and

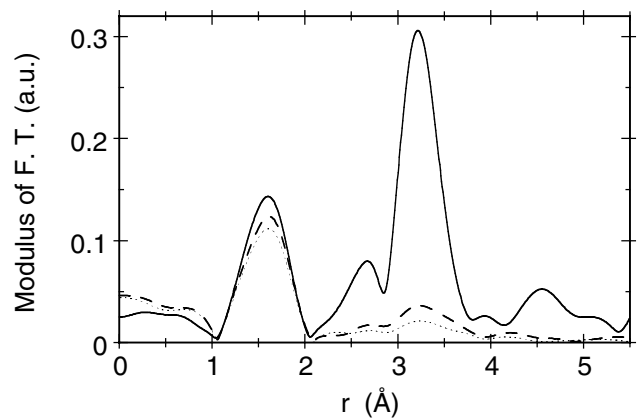


FIG. 1. Moduli of Fourier transforms of  $\text{Ag}_2\text{O}$  EXAFS at selected temperatures: 7 K (continuous line), 300 K (dashed line), and 500 K (dotted line).

2nd coordination shells. The corresponding values  $\delta C_i^*$  of the *real* distribution of distances were obtained assuming a photoelectron mean free path  $\lambda = 8 \text{ \AA}$ ; the use of the *ratio method* allows one to neglect the dependence of  $\lambda$  on the photoelectron wave number [15,16]. Absolute values of the thermal contribution to the 2nd cumulants,  $C_2^* \approx \langle \Delta u_{\parallel}^2 \rangle$ , were estimated by fitting correlated Einstein models to the experimental  $\delta C_2^*$  data [17]. The first two cumulants of both 1st and 2nd shells are shown in Figs. 2 and 3. The error bars represent the statistical uncertainty evaluated by reasonably varying the fitting intervals and cross-comparing the results from different files measured at the same temperature. Two main features are evident in Figs. 2 and 3: (a) The average 1st-shell Ag-O distance increases with temperature, while the average 2nd-shell Ag-Ag distance decreases. (b) The temperature dependence of the parallel MSRDS is very different, corresponding to bond-stretching effective force constants  $k_0 = 5.77 \text{ eV/\AA}^2$  and  $0.65 \text{ eV/\AA}^2$  for the 1st and the 2nd shell, respectively.

Let us consider in detail the 1st-shell results. The increment  $\delta C_1^*$  of the average Ag-O distance corresponds to a thermal expansion  $\alpha \approx 3 \times 10^{-5} \text{ K}^{-1}$ . According to Frenkel and Rehr [21], the thermal expansion due solely to the potential anharmonicity is  $a = -3k_3 C_2^*/k_0$ , where  $k_0$  and  $k_3$  are the 2nd and 3rd order force constants. In the present case of  $\text{Ag}_2\text{O}$ , the value  $k_0 = 5.77 \text{ eV/\AA}^2$  was determined from the Einstein fit to  $\delta C_2^*$ . A value  $k_3 = -5.8 \text{ eV/\AA}^3$  was obtained by fitting the temperature dependence of the third cumulant as expressed by Eq. (18) of the Frenkel and Rehr paper [21] to the experimental  $\delta C_3^*$  values. The resulting  $\delta a$  values, shown in Fig. 2 as crossed squares, correspond to an average thermal expansion  $\alpha \approx 1.8 \times 10^{-5} \text{ K}^{-1}$ . The contribution of zero point vibrations, here subtracted, amounted to about  $0.01 \text{ \AA}$ .

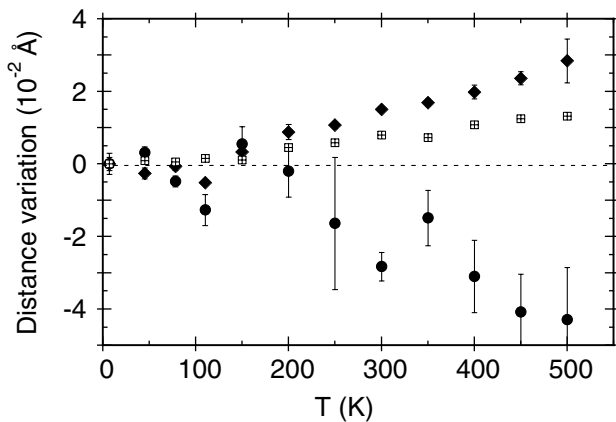


FIG. 2. Temperature dependence of the first EXAFS cumulants for the 1st-shell Ag-O (diamonds) and 2nd-shell Ag-Ag (circles). The crossed squares refer to the 1st-shell anharmonicity parameter  $a$ , defined in the text and determined from the third EXAFS cumulants.

The non-negligible discrepancy between  $\delta C_1^*$  and  $\delta a$  indicates that the nearest-neighbor motion is not purely librational, as would be expected for perfectly rigid tetrahedral  $\text{Ag}_4\text{O}$  units. According to Eq. (2),  $\delta C_1^* - \delta a = \delta \langle \Delta u_{\perp}^2 \rangle_{\text{tr}} / 2R_0$ , whence one can recover the absolute values  $\langle \Delta u_{\perp}^2 \rangle_{\text{tr}}$  by an Einstein fit [20]. The index “tr” indicates the translational contribution to the total perpendicular MSRDS; the librational contribution cannot be obtained solely from EXAFS measurements. The ratio  $\gamma = \langle \Delta u_{\perp}^2 \rangle_{\text{tr}} / \langle \Delta u_{\parallel}^2 \rangle$  is about 9 at high temperatures. At high temperature,  $\gamma$  should be 2 in the case of parallel-perpendicular isotropy, while a value 6 has been found for the 1st shell of germanium [20]. The high value of  $\gamma$  indicates that the Ag-O bond, which is rather stiff with respect to stretching, is much looser with respect to bending. This result is consistent with diffraction measurements on  $\text{Cu}_2\text{O}$  [25,26]. The low-frequency modes responsible for the bond bending monitored by EXAFS cannot be identified with RUMs; the translational character of the perpendicular MSRDS is instead a clear indication of a distortion of the  $\text{Ag}_4\text{O}$  tetrahedra. The relative motion is isotropic within the plane perpendicular to the Ag-O bond; by halving the projection  $\langle \Delta u_{\perp}^2 \rangle_{\text{tr}}$  one gets its component along one direction (crossed squares in Fig. 3), which is qualitatively consistent with the high values of the 2nd-shell parallel MSRDS. A quantitative evaluation of perpendicular and parallel MSRDSs of the 1st and 2nd shells, as well as of the uncorrelated MSDs measured by diffraction, would require a reliable knowledge of eigenvalues and eigenvectors of the dynamical matrix within the entire Brillouin zone and is beyond the aims of the present Letter.

The twelve 2nd-shell Ag atoms can be grouped into two sets [27]: six atoms (type A) are connected to the central atom via the 1st-shell oxygen atoms and belong to the same network; the remaining six atoms (type B) belong to the

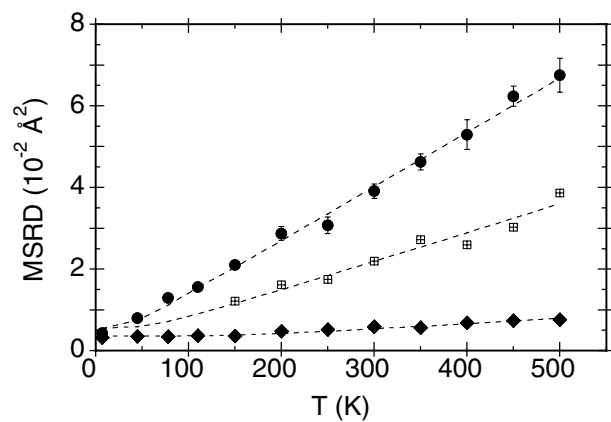


FIG. 3. Parallel MSRDSs  $\langle \Delta u_{\parallel}^2 \rangle$  for the 1st-shell Ag-O (diamonds) and 2nd-shell Ag-Ag (circles) distributions of distances. The crossed squares are the values of perpendicular translational MSRDS of the 1st shell,  $\langle \Delta u_{\perp}^2 \rangle_{\text{tr}} / 2$ . The dashed lines represent Einstein models.

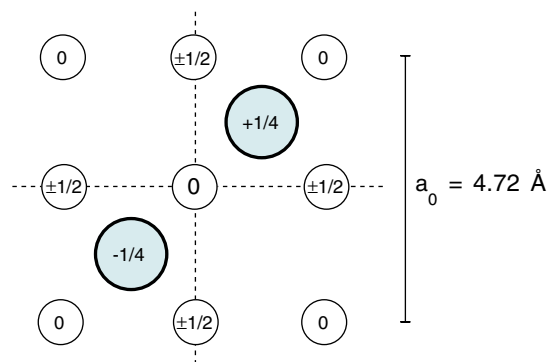


FIG. 4 (color online). Schematic representation of the absorber Ag atom and its first two coordination shells in  $\text{Ag}_2\text{O}$ , projected on the  $z = 0$  plane. Small and large circles represent silver and oxygen atoms, respectively; the numbers inside the symbols are the fractional  $z$  coordinates.

other network (Fig. 4). The 2nd-shell negative thermal expansion is consistent with recent diffraction measurements [6]. However, it cannot be attributed to the typical RUM mechanism, which contemplates the approaching between corner atoms belonging to different adjacent rigid units within the same network. Apart from the lack of rigidity of the basic units monitored by the 1st-shell EXAFS, the 2nd-shell distance refers to pairs of Ag atoms belonging to the same  $\text{Ag}_4\text{O}$  tetrahedra (type A) or to different networks (type B). Although no definitive conclusions can be drawn on the basis of present results, it seems reasonable that a relevant contribution to the 2nd-shell NTE comes from an average approaching of Ag atoms belonging to different networks, consistently with the presence of empty sites in the intermediate space.

In conclusion, a positive and a negative thermal expansion have been measured by EXAFS for the 1st-shell Ag-O and 2nd-shell Ag-Ag distances, respectively, in  $\text{Ag}_2\text{O}$ . It has been shown that a suitable cumulant analysis of EXAFS allows one not only to get information on the bond thermal expansion, but also to monitor the deformation of the basic units in framework structures. In the case of  $\text{Ag}_2\text{O}$ , evidence has been found of the lack of rigidity of the tetrahedral units: the large value of the 1st-shell ratio  $\langle \Delta u_{\perp}^2 \rangle_{\text{tr}} / \langle \Delta u_{\parallel}^2 \rangle$  is consistent with a strong effect of low frequency relative perpendicular translational motion. The 2nd-shell NTE cannot be explained in terms of a simple RUM model. The present results cannot be trivially generalized to other framework structures, in view of the different nature of chemical bonds which determine the rigidity of structural units. They however suggest that EXAFS could be advantageously used to get original information on local thermal expansion, complementing other experimental techniques and providing independent tests of theoretical models.

The authors are grateful to the staff of the Gilda beam line at ESRF for experimental assistance and to J. Purans

and A. Kuzmin for fruitful discussions. INFN financial support (Project No. BM08-01-199) is acknowledged.

\*Electronic address: fornasini@science.unitn.it

- [1] J. Zuo, M. Kim, M. O'Keefe, and J. Spence, *Nature (London)* **401**, 49 (1999).
- [2] J. Hallberg and R. C. Hanson, *Phys. Status Solidi* **42**, 305 (1970).
- [3] B. Prevot and C. Carabatos, *J. Phys. (Paris)* **32**, 543 (1971).
- [4] G. K. White, *J. Phys. C* **11**, 2171 (1978).
- [5] M. Ivanda, D. Waasmaier, A. Endriss, J. Ihringer, A. Kirfel, and W. Kiefer, *J. Raman Spectrosc.* **28**, 487 (1997).
- [6] G. Artioli and M. Dapiaggi (private communication).
- [7] J. S. O. Evans, *J. Chem. Soc. Dalton Trans.* **19**, 3317 (1999).
- [8] T. A. Mary, J. S. O. Evans, T. Vogt, and A. W. Sleight, *Science* **272**, 90 (1996).
- [9] V. Heine, P. R. L. Welche, and M. T. Dove, *J. Am. Ceram. Soc.* **82**, 1793 (1999).
- [10] B. T. M. Willis and A. W. Pryor, *Thermal Vibrations in Crystallography* (Cambridge University Press, Cambridge, 1975).
- [11] R. Downs, G. Gibbs, K. Bartelmehs, and J. M. B. Boisen, *Am. Mineral.* **77**, 751 (1992).
- [12] J. S. O. Evans, W. I. F. David, and A. W. Sleight, *Acta Crystallogr. Sect. B* **55**, 333 (1999).
- [13] M. G. Tucker, M. T. Dove, and D. A. Keen, *J. Phys. Condens. Matter* **12**, L425 (2000).
- [14] M. G. Tucker, M. T. Dove, and D. A. Keen, *J. Appl. Crystallogr.* **34**, 630 (2001).
- [15] G. Bunker, *Nucl. Instrum. Methods Phys. Res.* **207**, 437 (1983).
- [16] P. Fornasini, F. Monti, and A. Sanson, *J. Synchrotron. Radiat.* **8**, 1214 (2001).
- [17] P. Fornasini, *J. Phys. Condens. Matter* **13**, 7859 (2001).
- [18] G. Dalba, P. Fornasini, and F. Rocca, *Phys. Rev. B* **52**, 149 (1995).
- [19] O. Kamishima, T. Ishii, H. Maeda, and S. Hashino, *Solid State Commun.* **103**, 141 (1997).
- [20] G. Dalba, P. Fornasini, R. Grisenti, and J. Purans, *Phys. Rev. Lett.* **82**, 4240 (1999).
- [21] A. I. Frenkel and J. J. Rehr, *Phys. Rev. B* **48**, 585 (1993).
- [22] G. Dalba, P. Fornasini, F. Rocca, and F. Monti, *J. Non-Cryst. Solids* **293–295**, 93 (2001).
- [23] G. Dalba, P. Fornasini, and F. Rocca, *Phys. Rev. B* **47**, 8502 (1993).
- [24] J. Rehr, S. Zabinsky, and R. Albers, *Phys. Rev. Lett.* **69**, 3397 (1992).
- [25] A. Kirfel and K. Eichhorn, *Acta Crystallogr. Sect. A* **46**, 271 (1990).
- [26] T. Lippman and J. R. Schneider, *J. Appl. Crystallogr.* **33**, 156 (2000).
- [27] G. E. Kugel, C. Carabatos, and W. Kress, in *Ab Initio Calculation of Phonon Spectra*, edited by J. T. Devreese (Plenum Press, New York, 1983), pp. 101–115.